AIP | Review of Scientific Instruments

Measuring temperature-dependent activation energy in thermally activated processes: A 2D Arrhenius plot method

Jian V. Li, Steven W. Johnston, Yanfa Yan, and Dean H. Levi

Citation: Rev. Sci. Instrum. **81**, 033910 (2010); doi: 10.1063/1.3361130
View online: http://dx.doi.org/10.1063/1.3361130
View Table of Contents: http://rsi.aip.org/resource/1/RSINAK/v81/i3
Published by the American Institute of Physics.

Measuring temperature-dependent activation energy in thermally activated processes: A 2D Arrhenius plot method

Jian V. Li,[a] Steven W. Johnston, Yanfa Yan, and Dean H. Levi
National Renewable Energy Laboratory, Golden, Colorado 80401, USA

(Received 2 November 2009; accepted 22 February 2010; published online 29 March 2010)

Thermally activated processes are characterized by two key quantities, activation energy (E_a) and pre-exponential factor (ν_0), which may be temperature dependent. The accurate measurement of E_a, ν_0, and their temperature dependence is critical for understanding the thermal activation mechanisms of non-Arrhenius processes. However, the classic 1D Arrhenius plot-based methods cannot unambiguously measure E_a, ν_0, and their temperature dependence due to the mathematical impossibility of resolving two unknown 1D arrays from one 1D experimental data array. Here, we propose a 2D Arrhenius plot method to solve this fundamental problem. Our approach measures E_a at any temperature from matching the first and second moments of the data calculated with respect to temperature and rate in the 2D temperature-rate plane, and therefore is able to unambiguously solve E_a, ν_0, and their temperature dependence. The case study of deep level emission in a $Cu(In,Ga)Se_2$ solar cell using the 2D Arrhenius plot method reveals clear temperature dependent behavior of E_a and ν_0, which has not been observable by its 1D predecessors. © *2010 American Institute of Physics.* [doi:10.1063/1.3361130]

I. INTRODUCTION

Accurate measurement of activation energy E_a, pre-exponential factor ν_0, and in particular their temperature dependence is critical to understanding thermal activation processes such as electronic transitions, glass formation, and ion diffusion. To date, E_a and ν_0 are almost exclusively extracted using the universal Arrhenius equation[1]

$$\nu = \nu_0 \exp(-E_a/k_B T), \tag{1}$$

where k_B is the Boltzmann constant, T is the temperature, and ν is the rate measured at T. The standard Arrhenius plot method performs line fitting to the Arrhenius plot $-\ln(\nu)$ versus $1/T$, to extract E_a and ν_0 from the slope and intercept, respectively. Inherently, the standard Arrhenius plot method assumes that E_a and ν_0 are invariant over temperature. This assumption is valid when the Arrhenius plot is linear but it often fails in non-Arrhenius processes whose hallmark is a *curved* Arrhenius plot. The differential activation energy (DAE) method is commonly used to study such temperature dependent activation energy.[2] However, the differential activation energy is not the correct measurement of E_a when either one or both of E_a and ν_0 vary with temperature. Differentiating Eq. (1) shows that

$$-d[\ln(\nu)]/d\beta = E_a + \beta dE_a/d\beta - d[\ln(\nu_0)]/d\beta, \tag{2}$$

where $\beta \equiv 1/k_B T$ obviously contains two extra terms besides E_a. The root of difficulties for the classic Arrhenius plot based methods is the inherent conflict between the 1D nature of the experimental data $\nu(T)$ and the need to extract two independent 1D arrays $E_a(T)$ and $\nu_0(T)$ of the same size as $\nu(T)$. To circumvent this limitation, the 1D Arrhenius plot based methods either completely ignore or impose constraining temperature dependence to E_a or ν_0. Without such compromise, it is mathematically impossible to solve $E_a(T)$ and $\nu_0(T)$ independently from the information contained in the 1D Arrhenius plot. Many phenomena have been possible to understand exactly because of the temperature dependence of E_a and ν_0.[3,4] The lack of an effective method for studying arbitrary temperature dependence of E_a and ν_0 is in drastic contrast with the prospect that a wealth of physics is hidden in the vast number of non-Arrhenius processes.

II. METHOD

In this work, we propose a 2D Arrhenius plot method to overcome this fundamental limitation. Unlike its 1D predecessors, which measure only the first moment (e.g., peak position) of a measurable quantity X dependent both on T and ν to produce ν versus T in the 1D Arrhenius plot, this method distinctively exploits the second moment of X (e.g., the curvature of the peak). Sweeping X in the temperature-rate (T-ν) plane produces a 2D Arrhenius plot $-X(T,\nu)$. First, E_a at any temperature T is measured explicitly from matching the second moment of the mutually orthogonal scanning of $X(T,\nu)$ in the T-space and ν-space. Then, ν_0 at that temperature is uniquely solved according to Eq. (1). The unambiguous determination of $E_a(T)$ and $\nu_0(T)$ is made possible by expanding the raw experimental data from 1D to 2D and transformation of $X(T,\nu)$ scanning from ν-space to T-space due to the T-ν duality. A case study of deep level emission in a $Cu(In,Ga)Se_2$ solar cell demonstrates that the 2D Arrhenius plot approach reveals details of the temperature dependent behavior of E_a and ν_0 not possible by the classic Arrhenius plot based methods. These newly found details manifest observation of the Meyer–Neldel rule[5] by

[a]Electronic mail: jian.li@nrel.gov.

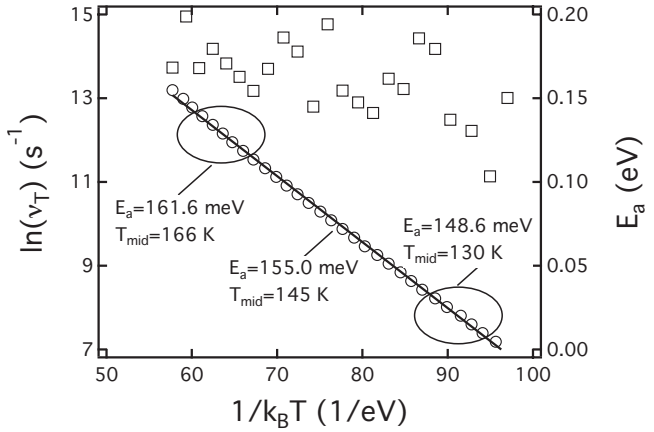

FIG. 1. The Arrhenius plot of the admittance spectroscopy data (○) taken from a $Cu(In,Ga)Se_2$ solar cell and the line fitting (line). The activation energies extracted by the standard 1D Arrhenius plot method from 30+ data points with midpoint temperature at $T_{mid} \sim 130$, 145, and 166 K are $E_a = 148.6$, 155.0, and 161.6 meV, respectively. The activation energy data extracted by the DAE method (□) barely show some temperature dependence but no detail can be extracted due to severe scattering.

varying temperature in a single sample only, in contrast with previous studies that require either multiple samples or additional physical quantities besides temperature.

We start with a critical inspection of the classic 1D Arrhenius plot based methods. In these methods, the rate quantity ν is usually the direct measurable as T is varied. A third parameter X is sometimes used as the direct measurable to extract ν from the first moment of X (e.g., peak position) as a function of T via isothermal or isorate scans. Regardless of how the data are obtained, the information retrievable from an Arrhenius plot is limited by its 1D nature, which leads to the aforementioned difficulties in the 1D Arrhenius plot based methods. Shown in Fig. 1 is a typical Arrhenius plot of 1D experimental data obtained from admittance spectroscopy[6] of a $Cu(In,Ga)Se_2$ solar cell. Fifty-nine data centered around 145 K are analyzed using the standard 1D Arrhenius plot method, which yields $E_a = 155.0 \pm 0.4$ meV. However, if we analyze the upper and lower 30 data points centered around 166 and 130 K, we would get E_a of 161.6 ± 0.6 and 148.6 ± 0.7 meV, respectively. All fittings have $R > 0.9995$. Clearly, E_a may vary significantly over temperature due to a very subtle curvature in the Arrhenius plot, which is not always easy to detect. E_a obtained by the DAE method (Fig. 1) exhibits severe scattering due to the numerical differentiation, from which no detail of temperature dependence can be deduced. The above analysis shows that the classic 1D Arrhenius plot based methods cannot unambiguously measure E_a and its temperature dependence.

However, our proposed 2D Arrhenius plot method is able to overcome the limitation of the 1D Arrhenius plot method. The key to our new method is to identify a measurable quantity X that depends on both T and ν. A 2D Arrhenius plot is obtained from the $X(T,\nu)$ surface acquired via a matrix scan of X in the T-ν plane. The physical information contained in $X(T,\nu)$, a 2D array of size $N \times M$ (N and M are the number of T and ν data points, respectively), is more than sufficient for solving two independent size-N 1D arrays $E_a(T)$ and $\nu_0(T)$. The solution of $E_a(T)$ and $\nu_0(T)$ hinges on this redundancy of information which has its origin in the T-ν duality. We first rearrange Eq. (1) into

$$T = E_a/k_B[\ln(\nu_0) - \ln(\nu)], \tag{3}$$

where ν is an experimental control parameter (i.e., not a mere measurable) independent of T. Equation (3) shows that sweeping in ν-space results in equivalently sweeping in T space, and visa versa. Consequently, varying either ν or T while keeping the other constant leads to equivalent variation of X in both the first and second moments. Consider two types of scans: (i) the isothermal scan $X(\nu)$ as ν is scanned with $T = T_{fix}$ fixed, and (ii) the isorate scan $X(T)$ as T is scanned with $\nu = \nu_{fix}$ fixed. These two scans independently delineate the activation behavior of the same quantity X and are probes of the same thermally activation process. Therefore one can use Eq. (3) to transform the isothermal scan $X(\nu)$ in ν-space to an equivalent scan $X(T_\nu)$ in T-space. Since the two physical unknowns E_a and ν_0 used in this ν-T transformation are related by Eq. (1) ($T = T_{fix}$, $\nu = \nu_{fix}$) and they are reduced to just one unknown. Assume E_a is the remaining unknown in the ν-T transformation, we recognize that the curvature in $X(T_\nu)$ varies with the value of E_a. The unique dependence of X on the intrinsic activation process described by Eq. (1) requires that the transformed scan $X(T_\nu)$ and the isorate scan $X(T)$ agree with each other near $T = T_{fix}$ in T-space. That is, there is not only agreement in the first moment, $X(T_\nu = T_{fix}) = X(T = T_{fix})$, but also agreement in the second moment [curvatures of $X(T_\nu)$ and $X(T)$ near $T = T_{fix}$]. The measurement of E_a at $T = T_{fix}$ is then accomplished by matching the curvatures of $X(T)$ to $X(T_\nu)$ without other arbitrary constraints such as invariance over temperature. Only the $X(T,\nu)$ data satisfying $(T - T_{fix}) \ll T_{fix}$ and $(\nu - \nu_{fix}) \ll \nu_{fix}$ should be used for the matching since $X(T)$ reflects E_a and ν_0 at all T, whereas $X(T_\nu)$ only reflects E_a and ν_0 at $T = T_{fix}$. Since the two scans are performed on physically independent variables, i.e., mutually orthogonal, they do not have measurement related correlations. Once E_a is measured, ν_0 is solved from Eq. (1). The 2D Arrhenius plot method thus unambiguously resolves E_a and ν_0 at $T = T_{fix}$. Repeating the above procedure for different T_{fix} yields the temperature dependent $E_a(T)$ and $\nu_0(T)$.

The 2D Arrhenius plot method is general since the duality between the activating energy source (k_BT) and the activated quantity (ν) is not specific to any physical process or experiment. However, it may not apply to certain processes where a measurable quantity X that depends on both T and ν cannot be identified or the rate ν cannot be experimentally controlled independent of T. The 2D Arrhenius plot method is readily applicable to transient capacitance techniques,[7] where X is the transient capacitance and the T-ν duality has been thoroughly discussed.[8] Other exemplar choices of measurable quantity X may include the permittivity,[9] the specific heat,[10] and mechanical susceptibility,[11] to name a few. Notice that the actual formula of $X(T,\nu)$ need not be explicitly known. The generality of the 2D Arrhenius plot method is further extended if one applies it to other activated process where the energy source is not of thermal nature, e.g., electric field F (T-ν duality changes to F-ν duality).

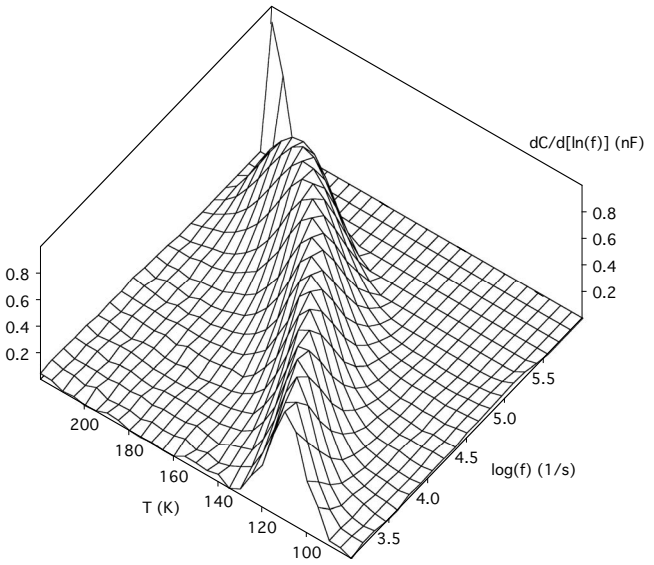

FIG. 2. The 2D Arrhenius surface plot of $X=dC/d[\ln(f)]$, where $f=\omega/2\pi$, due to deep levels in a Cu(In,Ga)Se_2 solar cell displayed against the temperature-frequency plane. The wire frame illustrates the isothermal and isofrequency scans.

We shall also make a distinction between the 2D Arrhenius plot method and the time-temperature superposition principle[12] method. The latter relies on the translational invariance of two isothermal scans (e.g., the frequency dependence of the elastic modulus of a polymer) taken at two different temperatures and matches one to the other (shifted in the abscissa by a shift factor) to construct a master curve. Its primarily purpose is to extend the total range of measurement time or frequency. In the less common cases where the William–Landel–Ferry equation[12] is not applicable, an activation energy can further be determined from the temperature dependence of the shift factor, that is, also using the 1D Arrhenius plot method. The 2D Arrhenius plot method, on the other hand, matches the isothermal scan to the isorate scan at a common (T,ν) point and therefore requires no translational invariance of isothermal (or isorate) scans.

III. RESULTS

We now show our case study for electronic transitions in Cu(In,Ga)Se_2. The 2D Arrhenius plot method is applied to admittance spectroscopy to investigate the deep level emission in a Cu(In,Ga)Se_2 solar cell. Since the emission rate of a deep level ν is related to the frequency ω at which the admittance is measured, we use $\omega(\omega_0)$ in place of $\nu(\nu_0)$. The conventional admittance spectroscopy analysis plots $\omega_{\max}$, the frequency at which the differential capacitance $dC/d[\ln(\omega)]$ peaks, against $1/T_{\text{fix}}$ and uses the Arrhenius plot to extract the activation energy and the attempt-to-escape frequency, as shown in Fig. 1. The capacitance C (or conductance G) due to the deep levels is a function of both the temperature T and frequency ω. The same is true for derivatives and combinations of capacitance and conductance, such as $dC/d[\ln(\omega)]$, dC/dT, and G/ω.

Figure 2 shows the 2D Arrhenius surface plot of $dC/d[\ln(\omega)]$ displayed in the T-ω plane. The experimental data are taken from a Cu(In,Ga)Se_2 solar cell fabricated using the three-stage process.[13] To minimize the temperature error, the temperature of the device is taken from a silicon diode attached directly to the top of the device. The admittance is measured using an Agilent 4294A impedance analyzer. Let us denote the isothermal scan $(T=T_{\text{fix}})$ $X(\omega)$ and the isofrequency scan $(\omega=\omega_{\text{fix}})$ $X(T)$. $X(\omega)$ is transformed into the T space to generate $X(T_\omega)$ via Eq. (3) where E_a varies freely and ω_0 varies accordingly due to Eq. (1) with $T=T_{\text{fix}}$, $\omega=\omega_{\text{fix}}$. For analysis convenience, T_{fix} and ω_{fix} are chosen to be at the peak of $X(T,\omega)$. E_a is determined by adjusting E_a so that the curvatures of $X(T)$ and the transformed scan $X(T_\omega)$ match each other as shown in Fig. 3. ω_0 for $T=T_{\text{fix}}$ is then solved from Eq. (1) with $\omega=\omega_{\text{fix}}$. Repeating this procedure for different T_{fix} yields the temperature dependent $E_a(T)$ and $\omega_0(T)$.

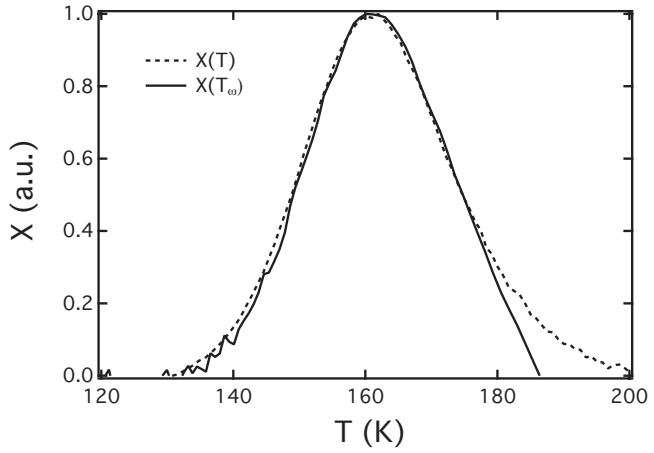

FIG. 3. The transformed isothermal scan $X(T_\omega)$ and isofrequency scan $X(T)$ taken from a Cu(In,Ga)Se_2 solar cell. The raw scans are taken at $T_{\text{fix}}=161.1$ K and $\omega_{\text{fix}}=300\,732$ s^{-1}, respectively. The deep level energy of 163 ± 3 meV is calculated using $\omega_0=2.0\times10^{10}$ s^{-1}.

In Fig. 4 we show the $E_a(T)$ and $\omega_0(T)$ for the same Cu(In,Ga)Se_2 sample extracted by the 2D Arrhenius plot method. The deep level energy E_a, as well as ω_0, depends strongly on temperature. The capture cross section increases almost exponentially with temperature even after considering

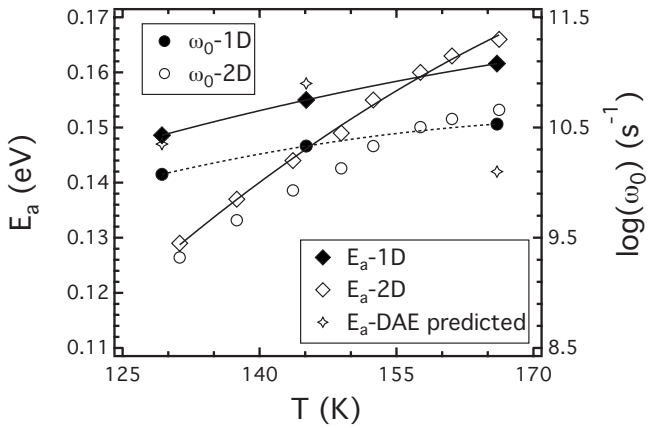

FIG. 4. $E_a(T)$ and $\omega_0(T)$ for deep levels in a Cu(In,Ga)Se_2 solar cell extracted by the 2D Arrhenius plot method (E_a-2D and ω_0-2D are plotted together with E_a-1D and (ω_0-1D extracted by the 1D Arrhenius plot method in Fig. 1. The lines are third order polynomial fitting to provide visual guidance. Also shown are the predicted E_a and ω_0 values (E_a-DAE predicted) by the DAE method according to Eq. (2).

the T^2 dependence embedded in ω_0 due to the effective density of states and thermal velocity of carriers. This suggests that multiphonon emission, as opposed to Auger and cascade mechanisms, is the most probable capture mechanism.[3] Since ω_0 extracted by the 2D Arrhenius plot method already includes its temperature dependence due to the corresponding capture mechanism, as opposed of being forced independent of temperature in a 1D Arrhenius plot method, E_a does not include contribution from the energy barrier that a carrier has to overcome during filling.[3] The temperature dependence of E_a still contains contribution of $2k_BT$ due to the effective density of states and thermal velocity of carriers. After discounting $2k_BT$, E_a still increases significantly with temperature. This is possibly due to the lattice dilation[15] in a Cu-poor nonstoichiometric $Cu(In,Ga)Se_2$. It should be noted that the previous studies on temperature dependent E_a and capture cross section all employ a separate experiment,[3,14,15] i.e., such information is not obtainable from 1D Arrhenius plot method alone.

Using third order polynomial fitting to estimate the temperature derivative of E_a and ω_0, we are able to predict E_a and ω_0 values extracted by the DAE method according to Eq. (2). As shown in Fig. 4, the predicted DAE values are very close to those measured by the 1D Arrhenius plot method at 130 and 145 K. This is an explicit demonstration of how the temperature variations in E_a and ω_0 result in the discrepancy in the estimate of E_a by the classic 1D Arrhenius plot method. It also provides a direct confirmation that $E_a(T)$ and $\omega_0(T)$ determined by the 2D Arrhenius plot method contains the true temperature dependence of these quantities in that temperature range and can be used to correct the intrinsic error due to the classic 1D Arrhenius plot method. The large discrepancy between the predicted DAE values and those measured by the 1D Arrhenius plot method at 166 K is possibly due to the lower signal-noise ratio (hence poorer peak fitting quality) and the fact that the measured data are in fact averaged across a wide range 167 ± 15 K.

Furthermore, using the E_a and ω_0 data extracted by the 2D Arrhenius plot method, a linear relationship is observed between $\ln(\omega_0)$ and E_a (shown in Fig. 5). This is a manifestation of the Meyer–Neldel rule for a deep level in the same sample ($T_{iso}=139\pm4$ K) with only temperature changed, in contrast with previous studies[5] where the activation energy is usually varied either by specially preparing a number of different samples or by varying certain parameters other than temperature on the same sample. The 2D Arrhenius plot method therefore dramatically simplifies study of Meyer–Neldel rule related phenomena, which hitherto required either multiple samples or additional measurements of quantities besides temperature. Due to the same poor signal-noise ratio at higher temperatures seen in Fig. 4, a slight sublinear deviation from the Meyer–Neldel rule is observed at high activation energies.

It is clear from the above discussion that the 2D Arrhenius plot method has substantial advantages over the classic 1D Arrhenius plot method, particularly for non-Arrhenius processes. In Arrhenius processes, in which the temperature dependence of E_a is small, both the 1D and 2D Arrhenius plot methods give similar results, validating the 2D Arrhenius plot method. For example, we also applied the 2D Arrhenius plot method to a GaAsN solar cell, which exhibits little non-Arrhenius behavior, and obtain the deep level energy of 336.4 ± 5.3 meV between 175 and 245 K (data not shown). This is consistent with that obtained from the 1D Arrhenius plot method (338.4 ± 3.4 meV). The deep level in the single crystalline GaAsN material is probably due to a discrete defect (hence a single emission rate) whereas those in the polycrystalline CIGS material may be due to a broadened distribution of defects (hence a distribution of emission rates). If the measurable quantity X fully reflects such distribution in the defect energy, then the temperature dependences of E_a and ν_0 are expected to contain contribution, or skewed, due to this nondiscrete nature. In the GaAsN and CIGS admittance spectroscopy data studied in this work, we observe full-width-half-maximum widths of the defect density of states ~40 and 30 meV, respectively. These values are close to the sampling width ($\sim 2k_BT$) in energy imposed by the admittance spectroscopy experiment.[16] The intrinsic energy linewidths of defect distribution in both materials are smaller than the measured values, which preclude a detailed study on the contribution of nondiscrete energy distribution to the non-Arrhenius activation using the existing data. A further investigation on thermal activation behavior due to broader energy distribution is underway.

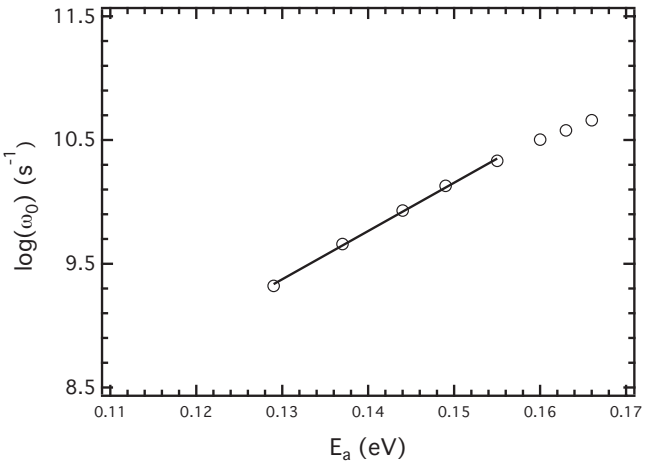

FIG. 5. The attempt-to-escape frequency plotted against the deep level energy (from Fig. 4) indicates that the Meyer–Neldel rule is obeyed with $T_{iso}=139\pm4$ K derived from linear fitting (solid line) except for some deviation at high temperature.

IV. CONCLUSIONS

In conclusion, we formulated a 2D Arrhenius plot method to resolve the temperature dependent E_a and ν_0 of a thermally activated process. Through a temperature-rate transformation based on the Arrhenius equation, E_a for a specific temperature is measured by matching the first and second moments of the isothermal and isorate scans of an observable $X(T,\nu)$. ν_0 at that temperature is then solved from the Arrhenius equation. In the case study of a $Cu(In,Ga)Se_2$ solar cell, our new method reveals that both the deep level energy and the attempt-to-escape frequency increase significantly with temperature. Such accurately detailed behavior could not possibly be obtained by the classic 1D Arrhenius

plot based methods. Furthermore, the relationship between the temperature dependent E_a and ν_0, obtained from a deep level in the same sample by temperature variation only, provides a significantly simplified method to study the Meyer–Neldel rule.

ACKNOWLEDGMENTS

The authors thank Dr. R. S. Crandall for insightful discussions and Dr. I. Repins for the $Cu(In,Ga)Se_2$ sample.

[1] S. Arrhenius, Z. Phys. Chem. **4**, 226 (1889).
[2] I. Vattulainen, J. Merikoski, T. Ala-Nissila, and S. C. Ying, Phys. Rev. Lett. **79**, 257 (1997).
[3] C. H. Henry and D. V. Lang, Phys. Rev. B **15**, 989 (1977).
[4] J. A. Van Vechten and C. D. Thurmond, Phys. Rev. B **14**, 3539 (1976).
[5] A. Yelon, B. Movaghar, and R. S. Crandall, Rep. Prog. Phys. **69**, 1145 (2006).
[6] D. L. Losee, J. Appl. Phys. **46**, 2204 (1975).
[7] D. V. Lang, J. Appl. Phys. **45**, 3023 (1974).
[8] S. Agarwal, Y. N. Mohapatra, and V. A. Singh, J. Appl. Phys. **77**, 3155 (1995).
[9] P. Lunkenheimer, U. Schneider, R. Brand, and A. Loidl, Contemp. Phys. **41**, 15 (2000).
[10] N. O. Birge and S. R. Nagel, Phys. Rev. Lett. **54**, 2674 (1985).
[11] G. Li, W. M. Du, X. K. Chen, H. Z. Cummins, and N. J. Tao, Phys. Rev. A **45**, 3867 (1992).
[12] Yu. S. Urzhumtsev, Polymer Mechanics **11**, 57 (1976).
[13] I. Repins, M. A. Contreras, B. Egaas, C. DeHart, J. Scharf, C. L. Perkins, B. To, and R. Noufi, Prog. Photovoltaics **16**, 235 (2008).
[14] P. Blood and J. J. Harris, J. Appl. Phys. **56**, 993 (1984).
[15] C. Lárez, C. Bellabarba, and C. Rincon, Appl. Phys. Lett. **65**, 1650 (1994).
[16] T. Walter, R. Herberholz, C. Muller, and H. W. Schock, J. Appl. Phys. **80**, 4411 (1996).